NONSTATIONARY ENERGY EXCHANGE BETWEEN LIGHT BEAMS IN A RESONANCE DYNAMIC HOLOGRAM

L.S. Korzun, T.V. Smirnova, and O.Kh. Khasanov

Institute of Solid–State Physics and Semiconductors, the Belorussian Academy of Sciences, Minsk
Received March 18, 1993

The authors study the kinetics of nonstationary energy exchange between reconstructing pulses and reconstructed waves in a resonance dynamic hologram. It is shown that the character of energy exchange between a reference beam and reconstructed waves essentially depends on the pulse areas of object beam and reconstructing pulse, their durations, and time lag between them, as well as on the stability of reference wave for small–scale disturbances of its transverse structure. It is found in particular that phase information about the object is distorted due to small–scale instability of the reconstructing pulses, even with no high spatial frequencies in the object spectrum.

1. INTRODUCTION

Prediction of phonon echo by U.Kh. Kopvillem and V.R. Nagibarov in 1963 (see Ref. 1) was of great fundamental and applied value. On the one hand, it boosted the development of such a lead as physics of coherent transient processes. On the other hand, the echo–phenomena are actively applied to coherent nonstationary spectroscopy[2–5] and resonance dynamic holography.[6–8] These are especially urgent problems now in connection with the development of real–time data processing systems as well as computers with optical memory.[9] This is favored by fast response and large memory capacity of the resonance dynamic holograms[10] (RDH's). Another lead is wavefront correction in high–power light pulses, in particular, wavefront reproduction (WFR) and phase conjugation (PC). Various nonlinear processes are employed to attain these ends including the four–wave interaction[11] (FWI). Its advantage is feasibility of the PC with simultaneous amplification of the phase conjugate signal. Photorefractive crystals as media, in which the dynamic holograms are recorded, are of considerable current use,[12] both the transmission and reflection holograms can be recorded in them depending on the experimental configuration.[13] To improve the efficiency of the PC, the intracavity FWI is often employed.[13] In a number of cases, however, resonant media appear to be more promising to record the dynamic holograms (DH's). They possess much stronger nonlinearity resulting in high energy sensitivity of such media. Thus for the DH's recorded in alkali metal vapor the sensitivity reaches $10^{-10} - 10^{-9}$ J/cm^2 (see Refs. 14–16). The response of the resonant media, determined, in particular, by the lifetime of the excited state (when the nonlinearity mechanism is associated with saturation of absorption) is many times faster than that of both photorefractive crystals and most other media. Moreover, the combination of fast response and sensitivity is a unique feature. The diffraction efficiency (DE) in the recording–reconstructing regime reaches 40% (Ref. 17), while the amplification factor for weak signals is 10^3 cm^{-1} (Ref. 18).

In addition, phase self–conjugation according to an off–axis cavity scheme[19–20] can be achieved in the resonant media. Recording and reconstructing can be performed both by simultaneous application of the object pulse and reconstructing pulse (RP) to the system of resonance atoms and by asynchronous excitation of such a system by these beams.[21] The DE of holograms then depends not only on the characteristics of interacting beams and spectroscopic parameters of the medium, but also on the time lag between the pulses. Depending on the employed experimental configuration, the RDH is recorded either in the regime of phonon echo[6] or in self–diffraction regime.[22,23] Since the wavelength of the optical beam is much shorter than the dimensions of the sample, the response of the medium to the exposure of the pulse must be taken into account in both cases.

In other words, the propagation of light pulses through the extended medium must be studied in the self–diffraction and echo regimes. Below we consider the RDH recording and reconstructing in the self–diffraction regime, since it sometimes provides higher diffraction efficiency of holograms, as compared to echo–holograms. At the same time many salient features of the RDH produced in the regime of self–diffraction are typical of echo–holograms.

Both the stationary and quasistationary self–diffraction regimes of recording have been studied in sufficient detail by now.[16–24] The nonstationary regime is of interest from the viewpoint of recording and reconstructing the holograms in the highly sensitive resonant media with ultra–short light pulses.[25–26] Such a technique makes it possible to improve the DE of the RDH, as compared to both the stationary and quasi–stationary cases.[27] Most studies[16,23,24,28,29] were concentrated on the spectral–energetic aspects of recording the RDH's. The problems of phase distortions of the transformed wavefronts have received much less attention so far. In particular, phase distortions due to self–action and interaction of recording beams during stationary recording of DH's were estimated in Refs. 24 and 28. It was demonstrated that the DH can be recorded with small phase distortions (below the Rayleigh criterion) and sufficient DE of about 5–10%.

Here we study the kinetics of nonstationary energy exchange between the RP and reproduced waves during the recording of the RDH as well as the effect of small–scale instability in the RP on the intensity of energy exchange and phase distortions in the reconstructed waves. This problem remains practically untackled within the scope of dynamic holography, although its urgency for propagation

0235-6880/93/07 466-09 $02.00

of solitons through extended resonant media was noted even in Refs. 30–32. It was found in particular that the transverse structure of a 2π pulse develops after it travels the distance of its own length $l = v\tau_p$, where v is the velocity of the soliton and τ_p is its duration.[32] The distortions depend on the size of the solution cross–section and may be great when cross–section radius $l_\perp \gg (\lambda l)^{1/2}$, where λ is the wavelength of the 2π pulse. It was demonstrated in Refs. 31 and 33 that small–scale distortions at exact resonance ($\Delta\omega = \omega_{21} - \omega = 0$, where ω_{21} is the frequency of the transition and ω is the carrier frequency of the pulse) are superposition of waist–like and snake–like distortions while the transition from one type of distortion to another takes place at large enough detunings from resonance. No stabilization occurs during the nonlinear stage of the development of instability of a long pulse ($\tau_p \gg T_2$, where T_2 is the rate of the irreversible transverse relaxation) when $l_\perp \gg (\lambda l_n)^{1/2}$, where $l_n = \alpha_n^{-1}$ and α_n are the coefficients of non–resonance absorption, nor multifold increase in the intensity of waveguide branches occurs.[32] Experiments demonstrated that the conjugate wave experiences the self–focusing instability during the FWI in sodium vapor.

2. QUASILINEAR REGIME OF RDH RECORDING

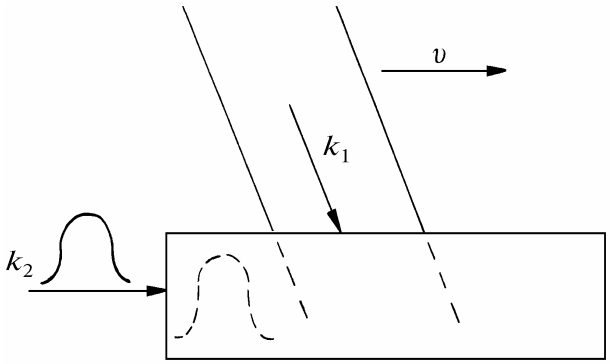

FIG. 1. Planned experimental configuration.

We consider, for simplicity, the following model configuration used for recording and reconstructing the RDH[23,34,35] (see Fig. 1). The object beam (OB) $E_{10}(x, z, t)$ scans line by line the side of the sample along the z axis, activating the system of resonance atoms to the state of superposition. The RP $E_2(x, z, t)$ approaches the sample from the same site. Its interaction with the polarization wave produced by the object wave results in the formation of a dynamic holographic lattice (polarization lattice[36]) while the diffraction of E_2 on this lattice produces reconstructed waves with reproduced wavefront (RWF) E_1 and conjugate wavefront (CWF) E_3, whose wave vectors being $\mathbf{k}_1$ and $\mathbf{k}_3 = 2\,\mathbf{k}_2 - \mathbf{k}_1$. Here $\mathbf{k}_{1(2)}$ is the wave vector of the object (reconstructing) wave. We assume that the durations of the local OB τ_{p1} and RP τ_{p2}, as well as the time lag between them τ_{12} are such that we may neglect the dissipative processes in the RDH. In contrast to the regime of running waves, scanning provides such conditions in extended media.[23]

We consider vapors of alkali metals as our system of resonance atoms, and assume that the durations τ_{p1} and τ_{p2} are such that the two–level approximation is valid. The Hamiltonian for that problem has the form

$$\mathcal{H} = \hbar\,\omega_{21}\,R_3 - \frac{d}{2}\left\{\sum_j R_+ \varepsilon_j(\mathbf{r},t)\exp i\left[\omega t - \kappa_j \mathbf{r} + \psi_j(\mathbf{r},t)\right] + \text{c.c.}\right\}, \tag{1}$$

where ω_{21} and ω are the frequency of the resonance transition and the RP carrier frequency, d is the dipole moment of the transition, $R_\pm = R_1 \pm i\,R_2$ and R_3 are the components of the energy spin $R = 1/2$, $\varepsilon_j(\mathbf{r}, t)$ is the envelope, and $\psi_j(\mathbf{r}, t)$ is the phase of the jth component of radiation. Then the self–consistent system of Maxwell–Bloch equations describing the interaction of the RP with the system of resonance atoms acquires the form

$$\dot{R}_+ = i\Delta\omega\,R_+ + i\frac{d}{\hbar}R_3\sum_j \varepsilon_j\,e^{-i(\mathbf{k}_j\mathbf{r} - \psi_j)} - \frac{R_+}{T_2}, \tag{2}$$

$$\dot{R}_- = -i\Delta\omega\,R_- - i\frac{d}{\hbar}R_3\sum_j \varepsilon_j\,e^{i(\mathbf{k}_j\mathbf{r} - \psi_j)} - \frac{R_-}{T_2}, \tag{3}$$

$$\dot{R}_3 = i\frac{d}{\hbar}\left\{R_+\sum_j \varepsilon_j\,e^{i(\mathbf{k}_j\mathbf{r} - \psi_j)} - R_-\sum_j \mathrm{e}_j\,e^{-i(\mathbf{k}_j\mathbf{r} - \psi_j)}\right\} - \frac{R_3 - R_0}{T_1}, \tag{4}$$

$$\sum_j \varepsilon_j\,e^{-i\,\mathbf{k}_j\mathbf{r}}\left[(\tilde{\mathbf{k}}_j\nabla)\,\tilde{\varepsilon}_j + \frac{n}{c}\frac{\partial\tilde{\varepsilon}_j}{\partial t} - i\Delta\kappa_j\tilde{\varepsilon}_j + \frac{i}{2\kappa}\Delta_\perp\tilde{\varepsilon}_j\right] = -\frac{2\pi i N\,d\omega}{c\,n}\int g(\Delta\omega)\,R_+(\Delta\omega,\,\mathbf{r},\,t)\,\mathrm{d}(\Delta\omega), \tag{5}$$

where $\tilde{\varepsilon}_j = \varepsilon_j\,e^{iw}$; $\tilde{\mathbf{k}}_j$ is the unit vector in the direction $\mathbf{k}_j$, $\Delta\kappa_j = \kappa_j - \omega\,n/c$, n is the refractive index, N is the number density of the resonance atoms, Δω is the detuning of the frequency of individual atom from the ensemble mean, $\Delta_\perp$ is the transverse Laplacian operator, and T_1 is the rate of the irreversible longitudinal relaxation. The third and fourth terms in the left–hand side of Eq. (5) are due to dispersion and diffraction of the interacting waves, respectively.

The initial conditions for the system of equations (2)–(5) describe preliminary excitation of the resonant medium by a square OB E_0 in the following way:

$$R_{\pm 0} = -i\frac{\gamma}{2}\sin\theta\,\exp\{\mp i(\mathbf{k}_1\mathbf{r} - \psi_1 - \Delta\omega\,\tau_{12})\},$$

$$R_{30} = -\frac{\gamma}{2}\cos\theta, \tag{6}$$

where $\gamma = 2\,t\,h\,[\hbar\,\omega_{21}(2\,\kappa_B\,T)^{-1}]$; κ_B is the Boltzmann constant, $\theta = \frac{2\,d}{\hbar}\varepsilon_1\,\tau_{p_1}$ is the local pulse area of the scanning OB, and the quantity ψ_1 carries phase information about the object. We assume for simplicity that $\psi_1 = \psi_0 + \kappa_\perp x$, where $\kappa_\perp$ is the spatial frequency in the object beam spectrum.

For quasilinear recording the superposition of interacting waves may be reduced to a certain effective field[34] with an envelope $\varepsilon_{\text{eff}} = \varepsilon_2 + \varepsilon_1 \cos(\delta\mathbf{k}_{21}\mathbf{r} - \delta\psi_{21}) + \varepsilon_3 \cos(\delta\mathbf{k}_{23}\mathbf{r} - \delta\psi_{23})$ where $\delta\mathbf{k}_{ij} = \mathbf{k}_i - \mathbf{k}_j$ and $\delta\psi_{ij} = \psi_i - \psi_j$. This system of equations (2)–(5) can be customarily transformed into a system of equations in the areas Φ_j and phases ψ_j of the interacting waves

$$\frac{\partial\Phi_1}{\partial z} = -\frac{\alpha}{2}\sin\theta\,[1 + \cos\Phi_2\, J_0(\Phi_1)\, J_0(\Phi_3)] \times$$

$$\times \cos(\psi_1 - \kappa_\perp x) \exp\left\{-\left(\frac{\tau_{12}}{2T_2^*}\right)^2\right\}, \qquad (7)$$

$$\frac{\partial\psi_1}{\partial z} = \frac{\alpha}{2}\sin\theta\,\frac{1 + \cos\Phi_2\, J_0(\Phi_1)\, J_0(\Phi_3)}{\Phi_1} \times$$

$$\times \sin(\psi_1 - \kappa_\perp x) \exp\left\{-\left(\frac{\tau_{12}}{2T_2^*}\right)^2\right\} + \frac{\kappa_\perp^2}{2\kappa} + \Delta\kappa, \qquad (8)$$

$$\frac{\partial\Phi_2}{\partial z} = -\frac{\alpha}{2}\cos\theta\, J_0(\Phi_1)\, J_0(\Phi_3)\, \sin\Phi_2, \qquad (9)$$

$$\frac{\partial\psi_2}{\partial z} = \Delta\kappa, \qquad (10)$$

$$\frac{\partial\Phi_3}{\partial z} = \frac{\alpha}{2}\sin\theta\,[1 - \cos\Phi_2\, J_0(\Phi_1)\, J_0(\Phi_3)]\cos\psi \exp\left\{-\left(\frac{\tau_{12}}{2T_2^*}\right)^2\right\}, \qquad (11)$$

$$\frac{\partial\psi_3}{\partial z} = \frac{\alpha}{2}\sin\theta\,\frac{1 - \cos\Phi_2\, J_0(\Phi_1)\, J_0(\Phi_3)}{\Phi_3} \times$$

$$\times \exp\left\{-\left(\frac{\tau_{12}}{2T_2^*}\right)^2\right\}\cos\psi - \Delta\kappa + \frac{\kappa_\perp^2}{2\kappa}, \qquad (12)$$

where $\psi = \psi_3 - 2\psi_2 + \kappa_\perp x$, $\alpha = 4\pi^{3/2} N d^2 \omega T_2^* (cn\hbar)^{-1}$, $\Phi_j = \frac{2d}{\hbar}\int_{\tau_{12}}^{\infty} \varepsilon_j(x, z, t)\, dt'$, T_2^* is the rate of the irreversible transverse relaxation, $J_0(\Phi_j)$ is the zero order Bessel function of the first kind, and $j = 1, 2, 3$.

It follows from Eq. (10) that $\psi_2 = \Delta\kappa z$, i.e., the run–on of the RP phase is accumulated along the propagation path. The rate at which the phases of the components ε_1 and ε_3 change is much higher than the rate of change of the envelopes, particularly close to the front face of the sample where Φ_1 and Φ_3 are small as compared to Φ_2. For $\Delta\kappa = 0$, $\kappa_\perp \ll \sqrt{2\kappa}$, and $\tau_{12} \ll T_2^*$ we have from Eq. (12)

$$\frac{\partial\psi}{\partial z} = -\frac{\alpha}{2}\sin\theta\,\frac{1 - \cos\Phi_2\, J_0(\Phi_1)\, J_0(\Phi_3)}{\Phi_3}\sin\psi.$$

It is easy to demonstrate (see Ref. 37) that the plane $\psi = 0$ must be stable in the phase space $\{\Phi_1, \Phi_2, \Phi_3, \psi\}$. Hence $\psi_3 = \psi + 2\psi_2 - \kappa_\perp x \to -\kappa_\perp x$ that is, the PC takes place. It may be similarly demonstrated that ψ_1 tends to the limit $\psi_1 = \pi + \kappa_\perp x$, which means the WFR. The phase locking of the interacting waves must be observed, which stabilizes the process of energy exchange between the RP and the reconstructed waves.[34] The energy is primarily transferred from the reference beam into the wave with RWF or CWF, depending on the pulse areas of the RP and OB. If the OB spectrum contains no high spatial frequencies, i.e., $\kappa_\perp \ll \sqrt{2\kappa}$, then small diffraction corrections cause no phase distortions of the waves being reconstructed. However, with such frequencies in the object beam spectrum, no phase locking occurs, and energy exchange is alternating and unstable in character that decreases the DE of the RDH.[35] It is of interest to investigate the most general case of diffraction and dispersion effects on the character of energy exchange and the quality of the RWF and CWF for arbitrary pulse areas of the OB and RP when the latter is strongly affected by the reconstructed waves ε_1 and ε_3.

3. THE EFFECT OF SMALL–SCALE INSTABILITY ON THE NONSTATIONARY ENERGY EXCHANGE BETWEEN THE INTERACTING BEAMS DURING HOLOGRAM RECORDING

As indicated above, the solitons in extended resonant media appear to be unstable towards small–scale distortions in their transverse structure. This naturally brings the question about the effect of distortions on the energy exchange and phase characteristics of the reconstructed waves. We consider the same configuration of RDH recording and reconstructing. In addition, we assume that the pulse areas of the OB and RP are such that the waves with RWF and CWF turn out to be comparable with the RP in their intensity due to energy exchange between the components. We then analyze the process of energy exchange between the RP and the waves with RWF and CWF as a function of the spatial frequency $\kappa_\perp$ recorded in the hologram, of the pulse areas θ and Φ_2^0, as well as of the value of $\Delta\kappa$. Here $\Phi_2^0 = \int_{-\infty}^{\infty} \varepsilon_2(\tau)d\tau = p\pi$ is the area of the RP and p is a certain positive constant.

The problem at hand is reduced to the analysis of the system of equations (2)–(5) with initial conditions (6). As before, the assumption is valid that $\tau_{p1}, \tau_{p2} \ll T_{1,2}$, in other words, that $T_{1,2} \to \infty$. The system of equations (2)–(5) may be reduced to a form convenient for its numerical analysis. We introduce new variables, related to the components of the polarization wave corresponding to the waves $R_\pm = \sum_{j=1}^{3} R_{\pm j}\, e^{\pm i\mathbf{k}_j \mathbf{r}}$ in the medium. After some transformations system (2)–(5) can be brought to the form

$$\ddot{R}_{+k} = i\Delta\omega\tau_p \dot{R}_{+k} - \frac{1}{2}R_{+k}\sum_j |E_j|^2 +$$

$$+\frac{1}{2}R_{-k}\left(E_\kappa^2 + 2E_{\kappa_1\neq\kappa}E_{\kappa_2\neq\kappa,\,\kappa_1}\right) +$$

$$+\left(\dot{R}_{+k} - i\Delta\omega\tau_p R_{+k}\right)\left(\sum_j \frac{\partial E_j}{\partial t}\right)\left(\sum_j E_j\right)^{-1}; \qquad (13)$$

$$\ddot{R}_{-k} = -i\Delta\omega\tau_p \dot{R}_{-k} - \frac{1}{2}R_{-k}\sum_j |E_j|^2 +$$

$$+\frac{1}{2}R_{+k}\left(E_k^{*2} + 2E^*_{\kappa_1\neq\kappa}E^*_{\kappa_2\neq\kappa,\,k_1}\right) +$$

$$+\left(\dot{R}_{-k}+i\Delta\omega\,\tau_p R_{-k}\right)\left(\sum_j\frac{\partial E_j^*}{\partial t}\right)\left(\sum_j E_j^*\right)^{-1}; \quad (14)$$

$$\frac{\partial E_\kappa}{\partial z}+\frac{\partial E_\kappa}{\partial t}-i\Delta\kappa l_n E_\kappa+\frac{i}{2}\frac{\partial^2 E_\kappa}{\partial x^2}=$$

$$=-i\frac{2\pi N d^2\omega\,\tau_p^2}{n\hbar}\int_{-\infty}^{\infty} g(\Delta\omega)R_{+k}(\Delta\omega,\mathbf{r},t)\,d(\Delta\omega),\ \kappa=1,2,3. \quad (15)$$

The system of equations (13)–(15) is in its dimensionless form. Amplitudes of the components E_k are expressed in units of $d\tau_p/\hbar$, the longitudinal coordinate z is in units of the absorption path length l_n, the transverse coordinate x is in units of $\sqrt{l_n/\kappa}$, and the time t is in units of l_n/c.

This system of equations was numerically solved by the net–point method.[38] To do that, uniform grids with steps h_x and h_z were specified over the $L_x\times L_z$ rectangular area. A characteristic approximation of the transfer operator was used and the step h_z was chosen to be equal to h_t. The values of E_k refer to the nodes of the grid $E^{\kappa}_{lj}=E(h_x l,\ h_z j,\ h_t\kappa)$ and $R_{\pm}$ is taken at the center of the straight line connecting the adjacent nodes along the z axis, i.e, $R^{\kappa}_{lj}=R(h_x l,\ h_z(j-1/2),\ h_t\kappa)$. To approximate the system to the second order $O(h_x^2,\ h_z^2,\ h_t^2)$, the unconditionally stable symmetric difference algorithms were used.[39] It is further assumed that the input RP has the shape $E_2(z=0)=E_0\,pch^{-1}(E_0(t-t_0))$, where E_0 is the peak value of E_2 at $t=t_0$.

To test the adequacy of the model, we studied numerically the propagation of a uniform planewave pulse of duration $\tau_p < T_{2,1}$ with the initial area 2π through a system of resonance two–level atoms without their preliminary excitation ($\theta=0$). The stability of such a soliton for small–scale disturbances of its transversal structure was studied. In analogy with Refs. 30–32, we assumed that the disturbance in the pulse transverse structure was sinusoidal with the period $l_\perp$ and was no more than 2% of the pulse amplitude.

Calculations showed that the small–scale instability of the RP wavefront is manifested already at the distance of four absorption lengths $z\sim 4\alpha_n^{-1}$. The pulse front is significantly deformed, and waveguide branches appear (Fig. 2).

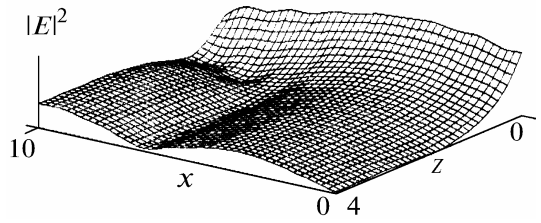

FIG. 2. Intensity distribution of the 2π*–pulse* $|E|_2^2(x, z)$ *for* $\tau_p = 1.5$.

During recording the dynamic holograms with $\theta\neq 0$ the energy exchange between the reconstructed waves and the RP depends strongly on the energy parameters and shapes of the OB and RP as well as on the shape of the RB. In analogy with the case of a single 2π – pulse we assume that the wave E_2 experiences distortions of its transverse structure, which is about 2% of the envelope. After this we impose the periodic boundary conditions assuming in analogy with Ref. 30 that the initial distortion is periodic in character. In this case, in contrast to Ref. 32, in addition to the arising diffractional lattice with the period $l_\perp$ we must take into account the lattice in the medium, on which the phase information is recorded.

It should be noted that the effect of the holographic lattice with the period $\kappa_\perp^{-1}$ on the development of the lattice of small–scale disturbances is not a trivial one. Apparently, such an effect is most pronounced at resonance between the two structures, when their periods coincide. It was particularly this case which was studied in our paper. It allowed us to consider the evolution of the RP within the limits of a single period assuming that the other parts of the RP cross–section developed independently.

Assuming that $l_\perp=\kappa_\perp^{-1}$, we consider energy exchange between the RP and the reconstructed waves as a function of θ and $\kappa_\perp$. The results are shown in Figs. 3–6. As the numerical analysis showed, the conditions for locking the phase of the reconstructed waves are met for small values of $\kappa_\perp$ when $\kappa_\perp\le 10\ \text{cm}^{-1}$. Figure 3 illustrates the evolution of the phase of the wave with RWF $\psi_1(r, t)$ for $\theta=\pi/5$, $\Phi_2^0=2\pi$, and $\kappa_\perp=1\ \text{cm}^{-1}$. The locking of phase ψ_1 at $x=0$ occurs at the point $\psi=\pi n$, as predicted in Ref. 23 on the basis of analytic estimates. With high spatial frequencies in the object spectrum ($\kappa_\perp>10\ \text{cm}^{-1}$) phase locking becomes impossible. It means that energy exchange between the interacting waves is unstable and high–quality reproduction of the phase of the object wave is possible only close to the front face of the sample ($z\sim 0.1\,\alpha_n^{-1}$). Moreover, the efficiency of the PC and WFR deteriorates.

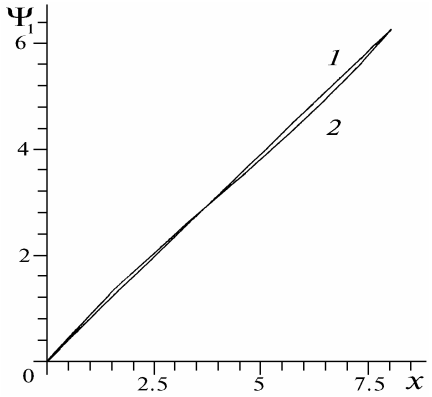

FIG. 3. Behavior of the wave with RWF $\psi_1(x)$ *for* $\theta=\pi/5$, $\Phi_2^0=2\pi$, *and* $\kappa_\perp=1\ \text{cm}^{-1}$. $z=0.2\,\alpha_n^{-1}$ *(1) and* $5.2\,\alpha_n^{-1}$ *(2).*

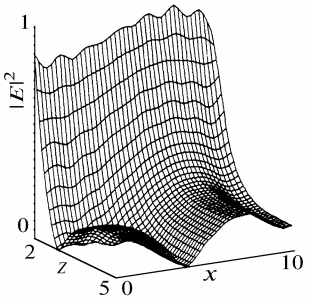

FIG. 4. Evolution of the RP wavefront for $\theta=\pi/5$, $\Phi_2^0=2\pi$, *and* $\kappa_\perp=1\ \text{cm}^{-1}$ *at time* $t=10.2$.

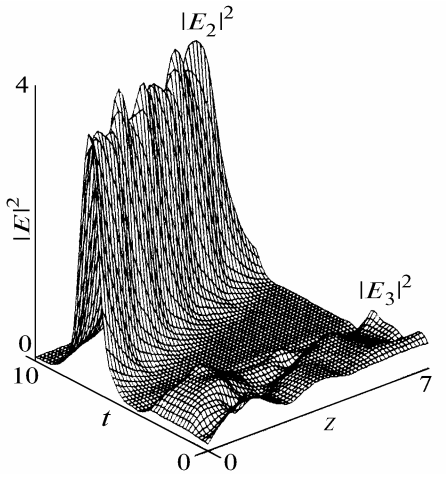

FIG. 5. Spatiotemporal distribution of the intensity of the reference beam and of the wave with RWF for $\theta = \pi/5$, $\kappa_\perp = 85\ \text{cm}^{-1}$, *and* $x = 0.5\ L_x$.

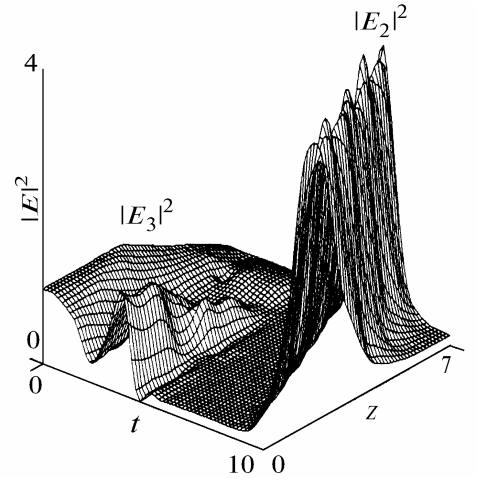

FIG. 6. Energy exchange between the RP and diffraction response with RWF for $\theta = \pi/5$, $\kappa_\perp = 1\ \text{cm}^{-1}$, *and* $x = 0.5\ L_x$.

Small–scale instability of the RP itself affects noticeably the phase distortions of waves produced at small $\kappa_\perp$ and the level of these distortions depends on the energy parameters and shapes of the object and reference waves. As seen from Fig. 3, the character of the dependence of ψ_1 noticeably changes as the distance from the front face of the sample increases. Even at short absorption lengths $z \sim 2\alpha_n^{-1}$ a deviation from the linear initial dependence $\psi_1|_{z=0}$ takes place due to the wavefront deformation of the pulse E_2. Figure 4 illustrates the evolution of the RP as the wave propagates through the medium at time $t = 10.2$ for $\theta = \pi/5$ and $\kappa_\perp = 1\ \text{cm}^{-1}$. Similar results are obtained for $\theta = \pi/60$ and $\theta = \pi/10$. However, distortions of phases ψ_1 and ψ_3 are less pronounced that is likely associated with the dependence of the arising small–scale instability of E_2 on the parameters of the OB. It is found that the character of energy exchange between the RP and the diffraction responses depends largely on the spatial frequency $\kappa_\perp$ and becomes nonmonotonic and unstable in character for large values of $\kappa_\perp$ (Fig. 5). However, as seen from Fig. 6, that nonmonotonic behavior is manifested also at small $\kappa_\perp$ ($\kappa_\perp \sim 1\ \text{cm}^{-1}$). Nevertheless, the wave E_1 reaches higher intensity in this case. With high spatial frequencies the character of energy exchange is determined by several factors. First, the instability of the RP wavefront towards the small–scale disturbances is manifested. Second, the phase run–on of the interacting waves changes periodically the phase relations between them. Finally, the instability of the wavefronts of the waves with RWF and CWF may manifest itself. Figure 7 shows the evolution of the wavefront of the wave E_1 in the medium for $\theta = \pi/5$, $\Phi_2^0 = 2\pi$, and $\kappa_\perp = 85\ \text{cm}^{-1}$ at time $t = 10.5$, clearly illustrating distortions in the transverse structure of the wave. The unstable character of energy exchange diminishes the intensity of the waves with RWF and CWF.

Studies of recording–reconstructing the RDH at arbitrary ratios of periods of the two diffractional lattices demonstrate that violation of resonance for $l_\cdot \neq k^{-1}$ strongly dampens the development of the small–scale instability of the RP. Nevertheless, stabilization of the energy exchange is lacking resulting in the lower DE of the holograms. Decreasing the level of the initial disturbances for $l_\cdot = k^{-1}$ somewhat weakens their effect on the RP stability, but the distortions in the transverse structure are still observed at large absorption lengths.

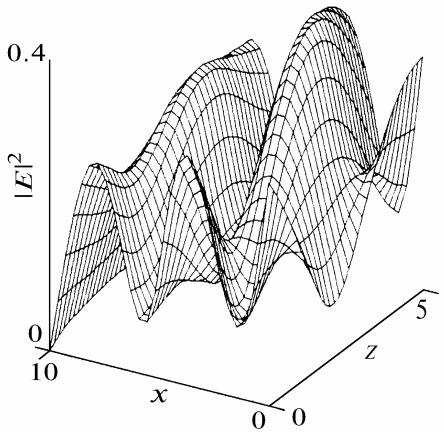

FIG. 7. Intensity distribution of the wave $|E|_1^2(x, z)$ *for* $\theta = \pi/5$, $\Phi_2^0 = 2\pi$, *and* $\kappa_\perp = 85\ \text{cm}^{-1}$ *at* $t = 10.5$.

A strong effect of RP dispersion not only on the character of energy exchange but also on the quality of the RWF and CWF should be noted. Even at $\Delta\kappa = 1\ \text{cm}^{-1}$ the transverse structure is distorted at $z = 0.1\alpha_n^{-1}$. The RP phase run–on deteriorates the conditions of energy exchange for E_1, E_3, and E_2. The exchange becomes alternating and unstable in character.

Thus the small–scale instability of RP in RDH and its dispersion substantially affect the wavefront reconstruction and conjugation. Even at low spatial frequencies phase information about the object is distorted due to the instability of the RP wavefront towards small–scale distortions of its transverse structure. Such distortions depend strongly on the pulse areas and durations of the OB and RP as well as on the time lag between them. Violation of the condition of phase locking (at $\kappa_\perp > 10\ \text{cm}^{-1}$) destabilizes the energy exchange between the RP and the reconstructed waves. The run–on of the phases of interacting waves in combination with the small–scale instability of their fronts significantly distorts the transverse structure of the waves with RWF and CWF. It is of interest to find out how such an instability manifests itself during recording of the DH's in the resonant media on homogeneously broadened spectral lines. To do that, we consider the conditions of experimental recording.[7,28,40]

4. QUASISTATIONARY RECORDING OF THE DH'S ON HOMOGENEOUSLY BROADENED SPECTRAL LINES

The above–considered configuration used for the RDH recording depends largely on the intensity and duration of the OB and RP as well as on the time lag between them, since holographic lattices are polarization ones by their nature. This suggests the use of the ultra–short pulses (USP) and provides rather high DE, as the above calculations show. At the same time the quasistationary regime of RDH recording on the homogeneously broadened spectral lines of vapor of alkali metals is deeply investigated.[15–17,28] However, the effect of small–scale distortions of the reference wave on the energy exchange during hologram recording in this regime remains practically unexplored, although its importance was pointed out even in the papers devoted to the stability of single pulses in the regime of enhanced transmittance.[32]

We consider recording of the 3D RDH's by strong and weak light pulses of one and the same carrier frequency simultaneously applied to the medium from one site. Theoretically that problem reduces to the analysis of a self–consistent system of equations (2)–(6) for $T_2 \ll \tau_{p2} \ll T_1$. Taking into account that the condition $\dot{R}_\pm = 0$ is satisfied, we may solve equations (2) and (3) for $R_\pm$ and by substituting them into Eq. (4), we obtain

$$\dot{R}_3 = \left(\frac{d}{2\hbar}\right)^2 \left\{ R_3 T_2 \left(\sum_j \tilde{\varepsilon}_j \, e^{i \mathbf{k}_j \mathbf{r}} \right) \times \right.$$

$$\left. \times \left(\sum_j \tilde{\varepsilon}_l \, e^{i \mathbf{k}_l \mathbf{r}} \right) (1 + i \Delta\omega T_2)^{-1} + \text{c.c.} \right\} . \qquad (16)$$

Upon integrating Eq. (16) over t within the limits $(\tau_{1,2}, \infty)$ taking into account the initial conditions $R_3(t = t_0) = R_{30} = -1/2$, we arrive at an expression for the component of the polarization wave

$$R_3 = R_{30} \exp\left\{ - \alpha \sum_j \int_{\tau_{12}}^{t} |\varepsilon_j|^2 \, dt' - \right.$$

$$- \alpha \sum_{l \neq j} \left[e^{-i(\mathbf{k}_l - \mathbf{k}_j)\mathbf{r}} \int_{\tau_{12}}^{t} \tilde{\varepsilon}_l \tilde{\varepsilon}_j^* dt' + \text{c.c.} \right] -$$

$$\left. i \Delta\omega T_2 \sum_{l \neq j} \left[e^{i(\mathbf{k}_l - \mathbf{k}_j)\mathbf{r}} \int_{\tau_{12}}^{t} \tilde{\varepsilon}_l^* \tilde{\varepsilon}_j \, dt' - \text{c.c.} \right] \right\} , \qquad (17)$$

where

$$\alpha^2 = \frac{d^2 T_2^2}{2\hbar^2 [1 + (\Delta\omega T_2)^2]} .$$

Using the well–known expression $\exp(\nu \cos x) = \sum_{m=-\infty}^{\infty} I_m(\nu) \exp(i m x)$ (here $I_m(\nu)$ are the modified Bessel functions) and considering the terms of the first order in the expansion ($m = 0, \pm 1$), after some transformations we reduce the considered problem to the following system of equations describing the envelopes of interacting waves

$$\frac{\partial E_j}{\partial z} + \frac{\partial E_j}{\partial t} + \frac{i}{2} \frac{\partial^2 E_j}{\partial x^2} = \frac{1 + i \Delta\omega T_2}{2} R_{30} \times$$

$$\times \exp\left\{ - \alpha \sum_j \int_{\tau_{12}}^{t} |E_j|^2 \, dt' \right\} \left\{ E_j I_0(-4\alpha |G_{21}|) \times \right.$$

$$\times I_0(4 \Delta\omega T_2 \alpha |G_{21}|) + E_l \exp[(-1)^j \cdot i \xi_{21}] \times$$

$$\times [I_0(-4\alpha |G_{21}|) I_1(4 \Delta\omega T_2 \alpha |G_{21}|) i^{(-1)^j - 1} +$$

$$\left. + I_0(4 \Delta\omega T_2 \alpha |G_{21}|) I_1(-4\alpha |G_{21}|) \right] \} , \qquad (18)$$

where $G_{lj} = \int_{\tau_{12}}^{t} |E_l E_j| \, e^{i(\psi_l - \psi_j)} \, dt'$, $\tan \xi_{lj} = \dfrac{\text{Im } G_{lj}}{\text{Re } G_{lj}}$, $j \neq l = 1, 2$.

System of equations (18) is written in its dimensionless form, and the units of the variables entering into it are the same as in Sec. 3. To solve this system numerically for the rectangular area $D = \{(z, x); 0 \le z \le L_z;\ 0 \le x \le L_x\}$, we specify the uniform grids and approximate the obtained equations at the nodes of these grids by the finite–difference algorithms analogous to the described above. It was assumed that the pulse of the reference wave applied to the input has the form $|E_2|^2 = \frac{1}{2}\left[1 + \tanh\left(t - \frac{z}{v} \right) / 2 \right]$ corresponding to the wave with enhanced transmittance.[32] The shape of the weak beam was assumed to be identical to the above. A sinusoidal distortion of the transverse structure, which did not exceed 2% of its envelope, was superimposed on the homogeneous planewave pulse at zero time.

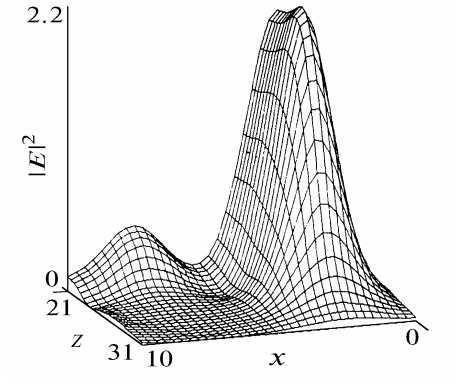

FIG. 8. Evolution of the wave front of the high–power beam at the nonlinear stage of the instability development ($t = 42$).

Numerical estimation of wavefront stability for a single pulse of indicated shape shows that the wavefront is distorted as the pulse propagates through the sample. The beam disintegrates into subpulses over the beam cross–section. Moreover, a certain increase in their intensity is observed. However, their maximum intensities at the developed stage of nonlinearity exceed the average ones by no more than 2.5 times (see Fig. 8). From the results of numerical computations we found that no stabilization takes place; however, the instability develops slower in case of non–optimal distortions determined by the value and sign of the detuning from resonance.[33] Distortions in the transverse structure are not so great when $0 < \Delta\omega T_2 \ll 1$, but when $\Delta\omega T_2 \geq 1$ (just the case analyzed in the present study) stabilisation is not observed while the rate of the increase of distortions is much higher, although, according to the estimates reported in Ref. 33, it contains a small numerical parameter.

Instability of the wavefront of the reference wave towards the small–scale distortions becomes pronounced for the waves being reconstructed resulting in their phase distortions and affecting the energy exchange. During the RDH reconstructing by long pulses (with the above–indicated relation between the frequency of the resonance transition and the pulse carrier frequency) the energy output for the components with RWF and CWF appears to be much lower than in the case of hologram recording–reconstructing by USP (see Fig. 9). This is due to relaxation of the induced macroscopic polarization carrying the information about the object in the course of its interaction with the high–power beam.

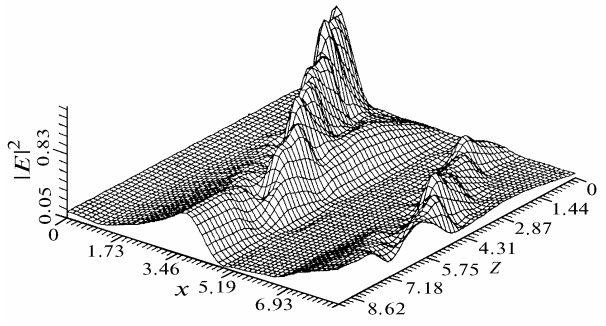

FIG. 9. Energy exchange between light pulses during the RDH reconstructing by long waves ($\kappa_\perp = 1\ \text{cm}^{-1}$ and $t = 45$).

CONCLUSION

Based on the above–discussed, we may conclude the following. The character of energy exchange between the reference beam and reconstructed waves in DH's in the extended resonant media essentially depends on the pulse areas of the OB and RP, on their durations, and on the time lag between them, as well as on the stability of the reference wave for small–scale distortions in its transverse structure. Because of instability of the RP towards these distortions, energy exchange is alternating and unstable in character, resulting in the lower DE of the RDH. During the DH reconstructing, the phase information about the object is distorted even in case with no high spatial frequencies $k_\perp$ in its spectrum. This is due to instability of the RP and the reconstructed waves towards the small–scale distortions of their wavefronts. These distortions are greatest if the spatial frequencies coinciding with the frequency of the distortion lattice are found in the object spectrum. The proper account of this factor provides the opportunity to minimize the arising distortions. When $\kappa_\perp$ is small ($\kappa_\perp < 10\ \text{cm}^{-1}$) and the dimensions of the medium do not exceed $4\alpha_n^{-1}$, phase locking of the interacting waves is observed, which stabilizes the process of energy exchange and provides the maximum DE of the RDH. Dispersion in the RP results in the lack of stabilization even under the above conditions.

During the DH reconstructing by long pulses the DE of interaction depends on the time lag between the pulses and on their durations, and is at maximum for maximum induced polarization. However, relaxation of that polarization noticeably diminishes the efficiency of energy exchange.

REFERENCES

1. U.Kh. Kopvillem and V.R. Nagibarov, Fiz. Met. Metalloved **15**, 313–315 (1963).
2. É.A. Manykin and V.V. Samartsev, *Optical Echo–Spectroscopy* (Nauka, Moscow, 1984), 272 pp.
3. U.Kh. Kopvillem and R.V. Saburova, *Para–Electric Resonance* (Nauka, Moscow, 1982), 224 pp.
4. V.A. Golenishchev–Kutuzov, V.V. Samartsev, and B.M. Khabibulin, *Pulsed Optical and Acoustic Coherent Spectroscopy* (Nauka, Moscow, 1988), 224 pp.
5. Yu.V. Naboikin, V.V. Samartsev, P.V. Zinov'ev, and N.B. Silayeva, *Coherent Spectroscopy of Molecular Crystals* (Naukova Dumka, Kiev, 1986), 204 pp.
6. E.I. Shtyrov and V.V. Samartsev, Phys. Status Solidi **45A**, 647–655 (1978).
7. P.A. Nefed'ev, Opt. Spektrosk, **57**, 889–893 (1984).
8. P.A. Nefed'ev, Opt. Spektrosk, **58**, 854–859 (1985).
9. U.Kh. Kopvillem, Izv. Akad. Nauk SSSR, Fiz. **37**, 2010–2021 (1973).
10. N.N. Akhmediev, V.S. Borisov, A.A. Kokin, et al., Elektronnaya Promyshlennost', No. 9, 56–59 (1984).
11. B.I. Stepanov, E.V. Ivakin, and A.S. Rubanov, Dokl. Akad. Nauk SSSR **196**, 567–569 (1971).
12. N. Kuchtarev, G. Dovgalenko, and V. Starkov, Appl. Phys. **A33**, 227–231 (1984).
13. O.N. Volkova and P.A. Zozulya, Kvant. Elektron. **16**, 1416–1421 (1989).
14. P.F. Liao, D.M. Bloom, and N.P. Economou, Appl. Phys. Lett., **32**, 813–815 (1978).
15. D.M. Bloom, P.F. Liao, and N.P. Economou, Opt. Lett. **2**, 58–60 (1978).

16. Koroljov A.E., Staselko D.I., Opt. Spektrosk. **57**, p. 299–305 (1984).
17. A.E Korolev. and D.I. Stasel'ko, in: *Holographic Techniques in Science and Technology* (Phys.–Techn. Inst. Publ. House, Leningrad, 1985), p. 104.
18. N. Tan–no, T. Hoshimija, and H. Inabo, IEEE J. Quant. Electron. **16**, 147–155 (1980).
19. P.A. Apanasevich, A.A. Afanas'ev, and S.Ya. Kilin, Kvant. Elektron. **12**, 863–865 (1985).
20. C.J. Gacta, J.F. Lam, and R.C. Lind, Opt. Lett. **14**, 245–247 (1989).
21. I.A. Nagibarova and O.Kh. Khasanov, Opt. Spektrosk. **55**, 125–128 (1983).
22. O.Kh. Khasanov, Opt. Spektrosk. **50**, p. 725–730 (1981).
23. O.Kh. Khasanov and P.A. Vlasov, J. Appl. Spectrosc. **44**, 32–37 (1986).
24. A.Ye. Korolev, V.N. Nazarov, and D.I. Stasel'ko, Zh. Tekh. Fiz. **55**, 111–118 (1985).
25. A.C. Afalas, T. Micropoulos, P. Simon, et al., Appl. Phys. **B46**, 363–368 (1988).
26. V.G. Bespalov, E.I. Zabello, A.E. Korolev, et al., in: *Abstracts of Reports at the Sixth All–Union Conference on Holography,* Vitebsk (1990), p. 88.
27. V.N. Abrashin, P.A. Apanasevich, A.A. Afanas'ev, et al., Kvant. Elektron. **12**, 546–552 (1985).
28. A.Ye. Korolev, V.N. Nazarov, and D.I. Stasel'ko, Pis'ma Zh. Tekh. Fiz. **12**, 732–737 (1986).
29. V.L. Vinetskii and N.V. Kukhtarev, Kvant. Elektron. **5**, 857–862 (1978).
30. P.A. Bol'shov, V.V. Likhanskii, and A.P. Napartovich, Zh. Eksp. Teor. Fiz. **72**, 1769–1774 (1977).
31. P.A. Bol'shov and V.V. Likhanskii, Zh. Eksp. Teor. Fiz. **75**, 2047–2053 (1978).
32. P.A. Bol'shov and T.K. Kirichenko, Kvant. Elektron. **7**, 2621–2626 (1980).
33. P.A. Bol'shov and V.V. Likhanskii, Appl. Phys. **19**, 221–225 (1979).
34. P.A. Vlasov, T.V. Smirnova, and O.Kh. Khasanov, Zh. Prikl. Spektrosk. **47**, 481–489 (1987).
35. T.V. Smirnova and O.Kh. Khasanov, Opt. Spectrosk. **66**, 200–204 (1989).
36. V.R. Nagibarov, I.A. Nagibarova, N.K. Solovarov, et al., Kvant. Elektron. **6**, 2175–2181 (1979).
37. V.S. Butylkin, A.E. Kaplan, Yu.G. Khronopulo, et al., *Resonance Interactions with Matter* (Nauka, Moscow, 1977), 352 pp.
38. A.A. Samarskii, *Theory of Difference Algorithms* (Nauka, Moscow, 1977), 653 pp.
39. Yu.N. Karamzin, A.P. Sukhorukov, and V.A. Trofimov, *Mathematical Modelling in Nonlinear Optics* (State Univ. Publ. House, Moscow, 1989), 154 pp.
40. A.E. Korolev and D.I. Staselko, Opt. Spectrosk. **58**, 147–152 (1985).